Journal of Applied Physics

Stress-induced phase transformation in shape memory ceramic nanoparticles

Cite as: J. Appl. Phys. **126**, 215109 (2019); https://doi.org/10.1063/1.5118818
Submitted: 08 July 2019 . Accepted: 21 November 2019 . Published Online: 04 December 2019

V. S. Raut, T. S. Glen, H. A. Rauch, H. Z. Yu, and S. T. Boles

Journal of Applied Physics ARTICLE scitation.org/journal/jap

Stress-induced phase transformation in shape memory ceramic nanoparticles

Cite as: J. Appl. Phys. **126**, 215109 (2019); doi: 10.1063/1.5118818
Submitted: 8 July 2019 · Accepted: 21 November 2019 ·
Published Online: 4 December 2019

V. S. Raut,[1] T. S. Glen,[1,a)] H. A. Rauch,[2] H. Z. Yu,[2] and S. T. Boles[1,b),c)]

AFFILIATIONS

[1]Department of Electrical Engineering, The Hong Kong Polytechnic University, Hung Hom, Kowloon, Hong Kong
[2]Department of Materials Science and Engineering, Virginia Polytechnic Institute and State University, Blacksburg, Virginia 24061-0002, USA

[a)]**Present address:** School of Physics and Astronomy, University of Edinburgh, Edinburgh EH9 3FD, United Kingdom.
[b)]**Author to whom correspondence should be addressed:** steven.t.boles@polyu.edu.hk
[c)]**Mailing address:** CF 608, Tang Ping Yuan Building, Department of Electrical Engineering, The Hong Kong Polytechnic University, 11 Yuk Choi Road, Hung Hom, Kowloon, Hong Kong.

ABSTRACT

Thermal treatment was observed to gradually transform the morphology of $Ce_{0.12}Zr_{0.88}O_2$ (CZ) powder: transitioning from having round edges, to exhibiting clear facets, to particle growth, as a function of increasing treatment temperature. The effect of the morphological changes in the powder on the extent of stress-induced phase transformation upon mechanical compression is reported. The physical changes in the average particle size and the residual levels of monoclinic content (MC) post thermal treatment between 300 °C and 1550 °C are in line with the expectations. However, the extent of transformation upon compression is found to greatly depend on the thermal history of the powder, and generally, post compression, MC can be split into two regimes. Powders heat-treated below ~1200 °C comprise regime 1, where post compression, MC increases as the preceding thermal processing temperature is increased. The increase in MC is despite the decreasing residual levels of the monoclinic phase in the CZ powder, which is caused by the thermal treatment. For the case of annealing above ~1200 °C (comprising regime 2), stress-induced transformation becomes exceedingly difficult and the extent of the transformation is significantly reduced. The vital role played by the particle shape alone can be leveraged in the development of new applications of shape memory ceramics.

INTRODUCTION

The reversible martensitic transformation observed in ceria doped zirconia ($Ce_{0.12}Zr_{0.88}O_2$, CZ) is of interest for various engineering[1–4] and research applications.[5–12] The underlying martensitic transformation is also observed in metallic systems such as nickel-titanium alloys (NiTiNOL),[13,14] Cu-Al-Ni microwires,[15] and Ni-Mn-Ga magnetic alloys.[16,17] Both stress and temperature can be used as independent stimuli for the material to undergo a transformation.[11] Such stress and thermally induced reversible martensitic transformations are the origin of the shape memory effect (SME) and the superelastic effect. Swain[9] first demonstrated these effects in a ceramic material, bulk zirconia samples partially stabilized by magnesia. A limitation to realizing the SME at the bulk scale in zirconia and other ceramic materials is due to their intrinsic brittle nature. Because of this, repeatable/cyclic behavior has been confined to only a few cycles.[18]

In order to circumvent the intrinsic limitations of ceramics at the bulk scale, the phenomena have recently been revisited with a focus on the nanoscale possibilities for this material and technology. For example, Lai *et al.*[19] demonstrably circumvented this limitation in micropillars (~1 μm diameter) of zirconia doped with either ceria (CZ) or yttria (YSZ). The pillars were observed to withstand strains as high as 7% for 50 cycles exhibiting the stress and temperature induced SME.[19] Further investigations into YSZ and titania doped zirconia micropillars by Zeng *et al.*[20] revealed a relationship between crystal orientation and martensitic transformation ability: The critical stress level required for nucleation and growth of the monoclinic phase was observed to vary systematically for different orientations during stress-induced transformation.

Orientation dependence was also investigated in 16% (mole) ceria doped zirconia particles by Du *et al.*,[21] which showed that oligocrystalline and monocrystalline particles could withstand cyclic superelasticity (over 100 for monocrystalline) but polycrystalline particles underwent fracture before sustaining the critical stress. Investigation in confined granular packing of CZ by Yu *et al.*[11] showed direct evidence of irreversible martensitic transformation in particles, and the transformed volume increased with loading.

Besides the size, the shape of the particle also plays a vital role in achieving different stress levels while undergoing compression in the bulk. The shape of the particle influencing the microstructure of bulk granular materials and the mechanical properties has been an interesting subject of investigation.[22–24] Generally, the shape of the particles is characterized by measuring the roundness and sphericity.[22,25–27] Several methods have been developed to characterize the sphericity and roundness of particles and subsequently relate them to the properties of the structures.[24,28–30] Athanassiadis *et al.*[22] found that the contacts produced with shapes having corners and straight facets made using hard resins during compaction showed a higher scaling exponent of effective modulus as compared to smooth-edged shapes like spheres. Though the sphericity of spheres and cubes is similar,[31] it is the facets that produce distinct contact types[32] contributing to a higher scaling exponent of effective modulus.[22]

Aside from granular systems, edges, facets, and corners are known to play an important role in controlling stress concentrations in fully densified structures. Chiu[33] (reported by Becher and Swain[34]) observed that stress concentration occurs on the corners and edges of the cuboidal shaped inclusion as well as grain corners[35] in ceramics, while similar observations have also been made in metallic systems.[36] The accumulation of various stresses at the edges and corners of cuboidal shaped inclusions and the concentration due to grain growth could provide the critical stress level required for nucleation in transformation.[34] Similar observations in sintered ceramics have been extensively studied in the past for the martensitic transformation, but the scope of these studies has been limited with respect to processing science.[37]

Energy damping techniques that utilize powders for the granular packing of SME ceramics, cermets,[11,38] or other composites must, therefore, consider both the particle sizes and shapes in the powder in order to have some desired property or functionality. This is more vital specifically in the context of scaling up SME ceramics for applications like energy and vibration damping wherein the size, scale, and few grains are major factors in designing the structure.[11]

In this investigation, we show that the pretreatment of CZ powder, i.e., thermal treatment, is critically important to the morphology of the material and that this has a large influence on the material's ability to undergo the stress-induced martensitic phase transformation. Moreover, the distinction of thermal treatment regimes with a characteristic particle evolution mechanism is the first step toward the deconvolution of the contributions of particle shape and size on the martensitic transformation behavior in CZ powders. Further issues regarding any subsequent change in the morphology of these ceramics (post sintering) can possibly be solved by techniques like spark plasma sintering in order to retain the microstructure[39,40] but are not explored in this study.

EXPERIMENTAL METHODS

Shape memory ceramic powders of 12% (mole) ceria doped zirconia (CZ) were received from Ganzhou Wanfeng Advanced Materials Tech. Co. Ltd. (China) with preliminary transmission electron microscopy (TEM) results suggesting that the powders were composed of monocrystalline particles of around 20 nm in diameter. Agglomerations in the CZ powder received from the supplier were removed by mixing with ethanol and heating the mixture on a hotplate at 150 °C. Separate samples of the refined, loose powder were then heat-treated in an alumina tube furnace at 300 °C–1300 °C (with 100 °C intervals) and 1550 °C. The furnace ramping rate was 10 °C/min, and the dwell time at peak temperatures mentioned above was 60 min. The subsequent cooling was not controlled but typically took between 5 and 8 h. One sample of CZ powder was processed at liquid nitrogen temperature to analyze the effect on monoclinic content (MC) due to martensitic transformation at that temperature. The sample was wrapped in aluminum foil and placed inside a vacuum flask in liquid nitrogen for 4 h. To study the effect of stress-induced phase transformation, 1 g from each of the powder samples after thermal processing is pressed at 40 kN (~250 MPa at the contact interface) to make pellets using a steel mold uniaxial pressing setup. The uniaxial pressing is done using a hydraulic press and is hand operated. Phase analysis was done using X-ray diffraction (XRD) spectra obtained by employing Bragg-Brentano (BB) and Parallel Beam (PB) features of the diffractometer for powders and their subsequent pellets, respectively. Rigaku SmartLab 45 kV 200 mA Cu K-alpha X-ray diffractometer with a wavelength (λ) of 0.154 nm was used to obtain the XRD spectra. The morphology of the CZ was characterized using TEM. Samples for TEM (Jeol 1200) analysis were prepared using refined CZ powder without thermal treatment and thermal treatment at 300 °C, 600 °C, 900 °C, 1100 °C, 1200 °C, and 1550 °C. The powder was dispersed in ethanol and placed in an ultrasonication chamber for 10–15 min. Few drops of the agitated mixture were dropped on TEM copper grid for imaging. The images were analyzed using ImageJ software. The sphericity of the particles was calculated by taking the ratio of minor axis to major axis of each particle in different samples processed at different temperatures. In the microstructural study of ceramics, the ratio of minor to major axis is referred to as aspect ratio[41] instead of sphericity.

RESULTS AND DISCUSSION

The morphology of the ceramic powder particles at different conditions was characterized by a comprehensive analysis using TEM images as shown in Fig. 1. Refined CZ powder with no thermal treatment reveals a quasispherical particle of less than 20 nm diameter as seen in Fig. 1(a). Thermal treatment at 300 °C [Fig. 1(b)] show no significant changes in the surface but some changes are seen in 600 °C [Fig. 1(c)] in the shape of the particle surfaces. The change in the surface becomes pronounced at 900 °C, and straight-faceted edges are seen in particles in Fig. 1(d). An increase in the size of the particles is also observed at 900 °C. The surface changes become more prominent at 1100 °C as the particles grow further in size. At 1100 °C [Fig. 1(e)], most of the particles have facets and straight edges. Further thermal treatment increases the particle size leading to fusion of the particles at several

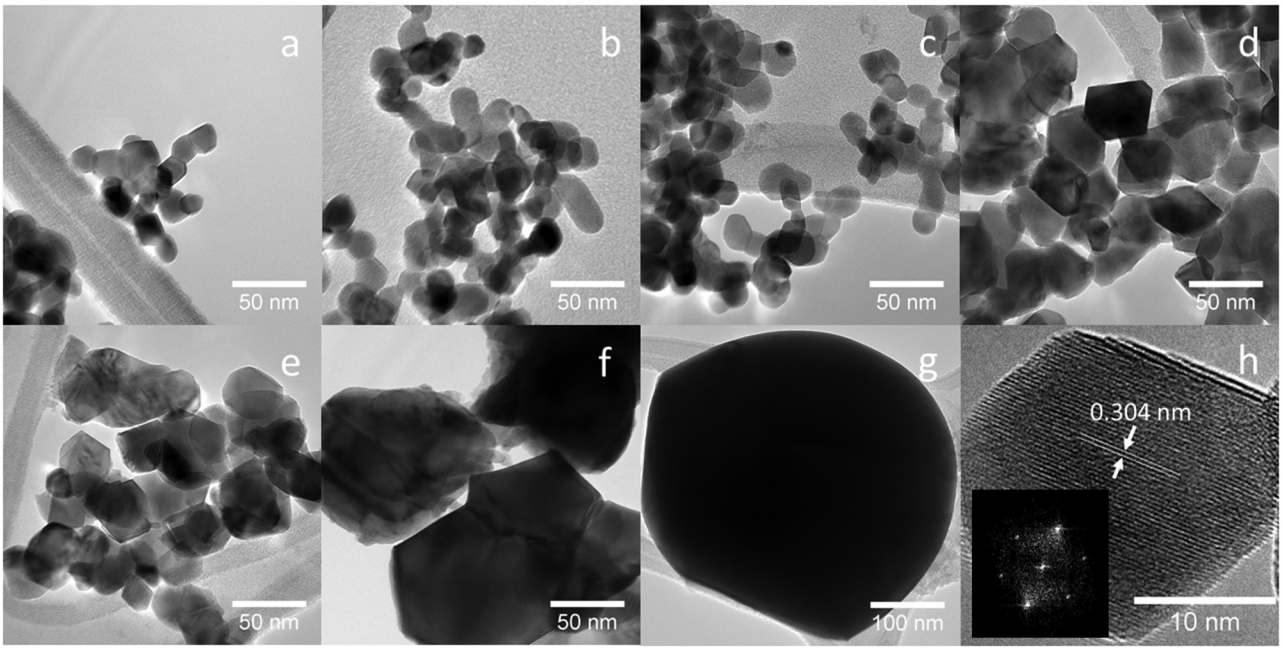

FIG. 1. TEM images of CZ powder processed at (a) no thermal treatment, (b) 300 °C, (c) 600 °C, (d) 900 °C, (e) 1100 °C, (f) 1200 °C, and (g) 1550 °C. (h) shows the HRTEM image and the inset is its FFT from a single CZ particle as received from the supplier.

instances of a particle to particle interface as seen at 1200 °C and at 1550 °C, i.e., Figs. 1(f) and 1(g), respectively. The high-resolution TEM image and Fast Fourier Transform (FFT) from a single particle were used to characterize the crystallinity of the CZ powder as received from the supplier as seen in Fig. 1(h). The single spots obtained from the FFT conclude that the particles are monocrystalline.

The increase in particle size as a function of processing temperature is evident in Fig. 1 and is measured by sampling ten particles from each TEM image. To ensure accuracy, several such TEM images are analyzed at different temperatures. The cross-sectional area of each particle in 2D is measured, and the diameter is calculated from the area shown (as a function of temperature) in Fig. 2. The diameter is observed to increase above 600 °C. It is quite likely that the particle size measured is a slight overestimate owing to the assumption that each particle is spherical in shape.

The phase analysis of zirconia consists of several tetragonal and monoclinic peaks out of which tetragonal (101) and monoclinic (111) and (11$\bar{1}$) are the peaks considered to have the strongest intensity.[42] Based on the relative intensities of these peaks, the MC in annealed and compressed powders is measured using Eq. (1) as observed in the XRD patterns,[7]

$$x_m = \frac{I_m(111) + I_m(11\bar{1})}{I_m(111) + I_m(11\bar{1}) + I_t(101)}. \quad (1)$$

The thermally induced phase transformation transforms the residual MC in the powders to the tetragonal phase and is shown in Fig. 3 whereby the MC calculated is observed to be reducing as the respective temperature of treatment increases. With the residual amount of the monoclinic phase, the volume of the phase present in each particle also decreases with increasing thermal treatment

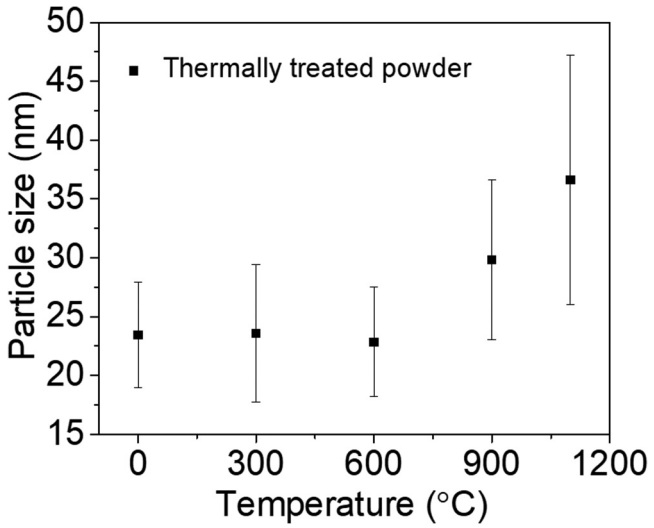

FIG. 2. Particle size shown as a function of temperature is measured from the projected area of ten particles per image and multiple such TEM images at different temperatures.

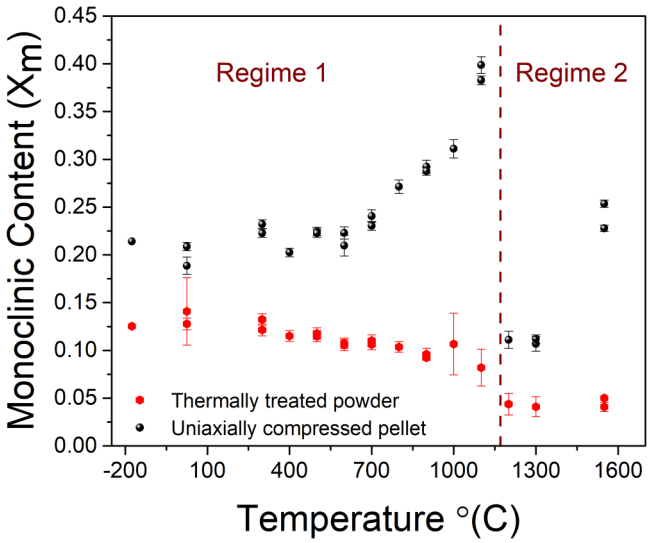

FIG. 3. Monoclinic content calculated in powder after heat treatment and in the pellet after compressing the processed powder. Error bars represent the absolute error calculated from the relative error as per error propagation (Calculation shown in the supplementary material). The dashed vertical line indicates the transition in the particle shape from regime 1 (quasispherical edges + straight-faceted edges) to regime 2 (sintering + particle growth).

temperature. Thus, the monoclinic phase available for growth during the transformation process is shrinking, and on this basis, it might be assumed that stress-induced transformation would be further limited due to the lack of MC. However, a divergent trend is observed between the monoclinic content in thermally processed powders and compressed pellets at lower temperatures. In this "regime 1," the MC due to stress-induced transformation increases significantly after 700 °C and is highlighted in Fig. 3. The MC in pellets showed incremental increases with the highest monoclinic content observed at a thermal treatment of 1100 °C.

Insights into the origin of the behavior in regime 1 can be corroborated by Chiu[33] (reported by Becher and Swain[34]) and by Garvie and Swain[43] In the study by Becher and Swain,[34] the influence of the grain size and residual stresses on the thermally induced martensitic transformation is investigated in *sintered CZ pellets*. Their results show a linear trend between the grain size and the amount of MC; larger grain sizes produce an increase in MC compared to small grain sizes while undergoing liquid nitrogen cooling (external thermodynamic driving force). In this case, the increased MC in larger grained samples was attributed to stress concentrations arising from thermal expansion anisotropy and strain mismatch at grain corners, amplifying the thermodynamic driving force for transformation compared to smaller grained samples that accumulate less stress. In other words, those samples with internal stress concentration sites—which happen to also have larger grain sizes—have an increased driving force for phase transformation, leading to higher MC. However, because this is explored with sintered pellets, the decoupling of grain size and geometric stress concentration is not addressed. In the case of Garvie and Swain,[43] the role of thermodynamics is explored, which considers the bulk chemical, strain, and interfacial energies. Even considering all such factors, it is noted that stresses that induce transformation can be amplified by sharp facets that may be dependent on the particle size.

The correlation between an increase in MC and an increase in grain size shows similarity to the findings in Figs. 2 and 3. However, the temperature range between 0 °C and 900 °C shows an increase in stress-induced martensitic transformation, despite little or no change in particle size and, therefore, the significance of the change in shape must be acknowledged.

The monoclinic content trend drops at 1200 °C and 1300 °C and increases again at 1550 °C, denoting "regime 2," as observed in Fig. 3. Also observed in Figs. 1 and 2 is the increase in particle size at 1200 °C and above due to thermal treatment. Because of thermal treatment, agglomerations of several particles or the interfaces of particles may develop bridgelike structures similar to necking. The formation of bridgelike structures between particles can be explained in a thermodynamic framework for surface energy-driven mass transport (i.e., necking and sintering) in order to comprehend the results shown in Fig. 1. In the case of faceting which is apparent at low treatment temperatures, it is a direct result of the intrinsic surface energy differences between different crystallographic planes of the zirconia lattice, where low-energy surfaces grow preferentially at the expense of high-energy interfaces. Extending this to the particle-particle contact points in a weakly bonded powder agglomerate results in a simultaneous reduction in concave surface area and the concavity of that surface, corresponding to an interparticle "neck" region. These processes occur through surface diffusion and happen relatively quickly at elevated temperatures. Once necking begins, it rapidly progresses to the point where necks are no longer appreciably concave and the particle-particle contact now more closely resembles a grain boundary and any further mass transfer will be slower as it will be driven by total surface energy reduction.

Necking would increase the area upon which the stress gets distributed during pressing, thereby reducing the local stress maxima during compression. Such necking in zirconia was observed by Boutz *et al.*[44] who found that below 1000 °C, the growth of grain size is slow and above this temperature, the grain size grows at an accelerated rate. Taking into account a shorter dwell time of 60 min in this investigation compared to 2–15 h in the investigation by Boutz *et al.*,[44] it is anticipated that the necking would set in at a higher temperature, evidently above 1200 °C, justifying the drop in MC in regime 2. The drop in MC in regime 2 has been explained in the context of necking based on the findings of Boutz *et al.*;[44] however, with the particle size and shape evolution observed in Fig. 1, necking can also be interpreted as particle-particle solid state diffusion marking the start of sintering.

The correlation between the stress-induced martensitic transformation and the change in the particle shape was explored primarily to investigate the effect of thermal treatment of particles on the subsequent stress-induced phase transformation. In regime 1, due to the thermal treatment, the particle shape is observed to evolve from round edges to straight-faceted edges while retaining the particle size as observed in Figs. 1 and 2. The sharp faceted edges, according to our hypothesis, exhibit enhanced stress concentration at particle to particle contacts as compared to more

round-edged particles at the same load. This leads to higher MC due to higher stress-induced phase transformation. In regime 2, the size of the particles was observed to increase greatly as compared to regime 1 leading to reduced stress exhibiting reduction in MC. At 1550 °C, the particle size is much larger and the MC thus observed is similar to regime 1. However, the findings of regime 2 require further experiments to gather comprehensive evidence, which is beyond the scope of this investigation.

Evolution in the shape of the particles in regime 1, as seen in the images presented in Fig. 1, was characterized by measuring the sphericity. Ideally, the sphericity of a sphere is 1 and for the cube is 0.87 measured by taking the ratio of the surface area of a sphere having the same volume as a particle to the surface area of the particle.[27] But the sphericity calculated using the ratio of minor to the major axis for both a sphere and a cube from a 2D image, i.e., a circle and a square, is 1. Similar sphericity for a sphere measured by both the methods and the surface being smooth would show minimal stress concentration under uniaxial compression. But the straight facets in a cube would produce contact types that show reduced area and experience stress concentration upon uniaxial compression.[22] Taking into consideration the difference in sphericity observed in cubes calculated using two separate methods, it is imperative to describe the faceting in particles in order to comprehend the effect of stress concentration on MC. Hence, the sphericity calculated by taking the ratio of minor and major axis using 2D TEM images is supplemented with the characterization of faceting.

The thermal treatment would change the particle surface resulting in facets, but in the absence of particle size growth, the aspect ratio would essentially stay the same. As the particle size increases and facets become more pronounced, combined with fusion with neighboring particles, the sphericity would reduce. However, this region would also show an increase in particle size due to particle fusion and as seen in both Figs. 1 and 2.

From the ten particles identified, the sphericity was calculated from the ratio of the minor axis to the major axis and is shown in Fig. 4. The ratio is observed to reduce as the thermal processing temperature increases, though no significant change is noted at 300 °C and 600 °C. By plotting MC as a function of sphericity, it is observed that as the sphericity reduces, the MC increases. Cropped images of particles from the TEM images in Fig. 1 are shown alongside the data points in Fig. 4 with the axis used to calculate the ratio.

As noted by Heffelfinger and Carter,[45] the process of faceting decomposes an existing surface into two or more surfaces. Taking into consideration the incremental thermal treatment on CZ in this study, the faceting evidenced here can be explained in this context: The as received CZ powder particles have smooth surfaces, with a range of thermodynamically stable and unstable facets, which will evolve as a function of the thermal treatment temperature., Herring[46] found that, besides the surfaces found on the equilibrium crystal shape, faceting will be observed in the form of hill and valley structures due to the consumption of these initial surfaces to form new ones.[45] The surface diffusion at high temperatures leads to the nucleation of individual facets, and this nucleation promotes the growth of more facets around it.[47] This is also consistent with Bonevich *et al.*,[48] who proposed a model whereby during the activation of surface diffusion in alumina

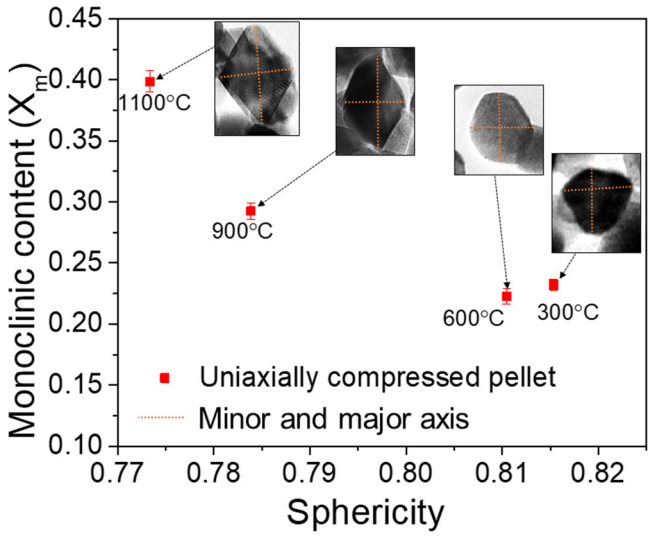

FIG. 4. The change in monoclinic content as a function of sphericity. Dotted lines on TEM images in the insets depict major and minor axes used to calculate the sphericity.

nanoparticles, atoms on the surface of the particle tend to have a higher degree of surface mobility, which leads to accelerated mass transport. The atoms move around the facets and contribute to their growth, as dangling bonds are energetically unfavorable.[48] The increase in the width of the facets increases the size, and these regions serve as nucleation sites for the growth of more facets developing hill and valley structures on the particle surface. This was elaborated by Heffelfinger and Carter[45] stating that the faceting grows by coarsening, wherein the driving force for the increase in the average width of the facet with time is surface free energy. Once formed, these facets and so-called "hill and valley structures" act as stress concentration sites that intensify the effects of the applied load and lead to more extensive stress-induced martensitic transformation as the precompression treatment temperature—and resultant faceting—is increased. Mullins[49] proposed a model that stated that the growth of the facets is governed by the power law, which varies depending upon the mass transport mechanism. Zirconia-based ceramics are well-known to be good ionic conductors at moderate temperatures,[50,51] which strongly supports a mass transport kinetic mechanism that enables the net reduction in surface free energy.

To further support the quantification of stress concentrations from edges and facets, instances where sharp or straight edges [900 °C—Fig. 1(d), cropped inset in Fig. 5(a)] were observed as opposed to a quasispherical edge [300 °C—Fig. 1(b), cropped inset in Fig. 5(a)] are sampled from the TEM image sets. The average number of faceted edges per particle was quantified by dividing the average with the total number of particles analyzed, i.e., 10 per image. The average number of such sharp edges per particle in the analyzed TEM images is observed to increase as a function of temperature and is shown in Fig. 5(a).

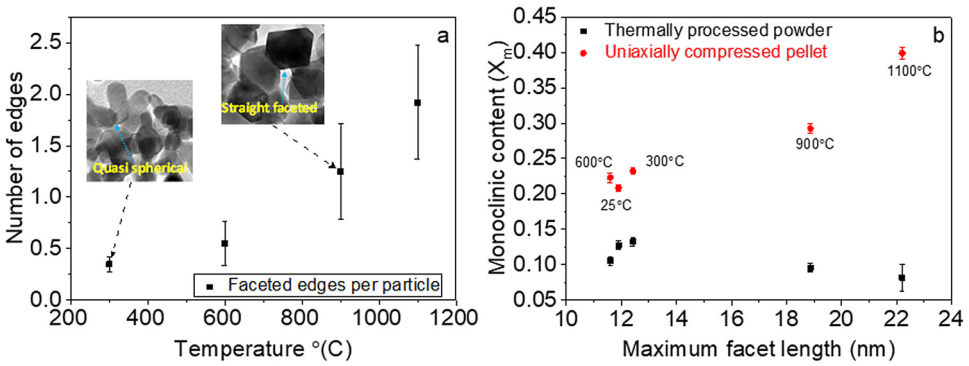

FIG. 5. The number of edges with straight facets per particle increases as a function of temperature in (a) and measurements taken from particles observed in TEM images show an increasing trend in monoclinic content as a function of maximum facet length in (b). Insets in (a) are from Fig. 1 and show the change in faceting at lower and higher temperatures.

The maximum length of the straight edges of the particle surface was measured and is shown as the maximum facet length in Fig. 5(b). The maximum length in particles was observed to increase as a function of temperature. The increase in length shows the gradual formation of sharp edges at the nanoscale, which would act as stress concentrators on the application of stress. The gradual evolution of edges from curved smooth surfaces to sharp faceted edges would increase the intensity of stress concentration. Further increase in the stress concentration would occur due to the increase in the length of the facets aiding higher growth of monoclinic phase.

It should be acknowledged that the effect of thermal treatment may also influence the residual strain in the particles, which, in turn, could impact the nucleation and propagation of a newly formed monoclinic phase upon loading. However, deciphering this role of strain, stress, and shape anisotropy would best be considered in future work as the materials and methods employed here do not allow for full deconvolution of their competing effects.

CONCLUSION

Thermal treatment on 12% (mole) ceria doped zirconia ($Ce_{0.12}Zr_{0.88}O_2$) powder reduced the ability for the powder to undergo a martensitic transformation, but it also changed the powder morphology. The change in morphology was characterized using TEM images that showed the evolution of particle surface from quasi-spherical edges to straight-faceted edges. The first regime showed a negative correlation between stress-induced and thermal-induced transformation. The monoclinic content is gradually increasing from 300 °C to 1200 °C (regime 1) beyond which (>1200 °C, regime 2), the growth of monoclinic content is limited. The increasing straight edges, corners, and facet length of the particles in regime 1 strongly support the presumption that sharp features evolve as a function of temperature. The sphericity and facets, combined or standalone, act as stress concentrators and aid the growth of monoclinic content during stress-induced transformation. In regime 2, the sudden drop and rise in MC form interesting results that demand further experiments and thus would be part of future work.

SUPPLEMENTARY MATERIAL

The error bars used to define the limits of the monoclinic content by taking into consideration the noise observed in XRD spectra were calculated using the error propagation method. A sample of the said calculation describing the method is included in the supplementary material.

ACKNOWLEDGMENTS

We would like to thank Dr. Mohammad H. Tahmasebi for his useful comments in preparing the manuscript and Ran Sijia for her help with TEM. Dr. S. T. Boles would like to acknowledge the funding support of internal projects "Novel Materials for Emerging Energy, Electronic and Photonic Devices" (No. 1- ZVGH), "Electrochemical Energy Storage Systems" (No. 1-ZVD2), and "In Situ Mechanical and Electrical Testing of Nanomaterials for Next Generation Electronic Devices" (No. G-YBLN/G-YBPQ) of the Hong Kong Polytechnic University.

The authors declare that they have no conflict of interest.

REFERENCES

[1]J. Chevalier, L. Gremillard, A. V. Virkar, and D. R. Clarke, J. Am. Ceram. Soc. **92**, 1901 (2009).
[2]A. Nespoli, D. Rigamonti, E. Villa, and F. Passaretti, Sens. Actuators A **218**, 142 (2014).
[3]L. Sun, W. M. Huang, Z. Ding, Y. Zhao, C. C. Wang, H. Purnawali, and C. Tang, Mater. Des. **33**, 577 (2012).
[4]A. T. Tung, B. H. Park, G. Niemeyer, and D. H. Liang, IEEE ASME Trans. Mechatron. **12**, 439 (2007).
[5]R. C. Garvie, R. H. Hannink, and R. T. Pascoe, Nature **258**, 703 (1975).
[6]M. V. Swain and R. H. J. Hannink, J. Am. Ceram. Soc. **72**, 1358 (1989).
[7]R. C. Garvie and P. S. Nicholson, J. Am. Ceram. Soc. **55**, 303 (1972).
[8]I. W. Chen and P. E. Reyes-Morel, J. Am. Ceram. Soc. **69**, 181 (1986).
[9]M. V. Swain, Nature **322**, 234 (1986).
[10]R. H. J. Hannink, P. M. Kelly, and B. C. Muddle, J. Am. Ceram. Soc. **83**, 461 (2000).
[11]H. Z. Yu, M. Hassani-Gangaraj, Z. Du, C. L. Gan, and C. A. Schuh, Acta Mater. **132**, 455 (2017).
[12]I. Karaman, B. Basaran, H. E. Karaca, A. I. Karsilayan, and Y. I. Chumlyakov, Appl. Phys. Lett. **90**, 172505 (2007).
[13]R. J. Wasilewski, Metall. Trans. **2**, 2973 (1971).
[14]J. W. Christian, *The Theory of Transformations in Metals and Alloys* (Pergamon, 2002).
[15]Y. Chen and C. A. Schuh, Acta Mater. **59**, 537 (2011).
[16]W. Liang, M. Zhou, and F. Ke, Nano Lett. **5**, 2039 (2005).
[17]D. C. Dunand and P. Müllner, Adv. Mater. **23**, 216 (2011).

[18]P. E. Reyes-Morel, J.-S. Cherng, and I.-W. Chen, J. Am. Ceram. Soc. **71**, 648 (1988).
[19]A. Lai, Z. Du, C. L. Gan, and C. A. Schuh, Science **341**, 1505 (2013).
[20]X. M. Zeng, A. Lai, C. L. Gan, and C. A. Schuh, Acta Mater. **116**, 124 (2016).
[21]Z. Du, X. M. Zeng, Q. Liu, C. A. Schuh, and C. L. Gan, Acta Mater. **123**, 255 (2017).
[22]A. G. Athanassiadis, M. Z. Miskin, P. Kaplan, N. Rodenberg, S. H. Lee, J. Merritt, E. Brown, J. Amend, H. Lipson, and H. M. Jaeger, Soft Matter **10**, 48 (2014).
[23]R. Kandasami and T. Murthy, *Geomechanics from Micro to Macro* (CRC Press, 2014), pp. 1093–1098.
[24]G.-C. Cho, J. Dodds, and J. C. Santamarina, J. Geotech. Geoenviron. Eng. **132**, 591 (2006).
[25]A. B. Yu and N. Standish, Powder Technol. **74**, 205 (1993).
[26]R. D. Hryciw, J. Zheng, and K. Shetler, J. Geotech. Geoenviron. Eng. **142**, 04016038 (2016).
[27]R. P. Zou and A. B. Yu, Powder Technol. **88**, 71 (1996).
[28]W. C. Krumbein and L. L. Sloss, *Stratigraphy and Sedimentation* (Freeman, 1951).
[29]T. P. Meloy, Powder Technol. **17**, 27 (1977).
[30]J. P. Hyslip and L. E. Vallejo, Eng. Geol. **48**, 231 (1997).
[31]Y. Li, Bull. Eng. Geol. Environ. **72**, 371 (2013).
[32]H. A. Rauch, Y. Chen, K. An, and H. Z. Yu, Acta Mater. **168**, 362 (2019).
[33]Y. P. Chiu, J. Appl. Mech. **44**(4), 587 (1977).
[34]P. F. Becher and M. V. Swain, J. Am. Ceram. Soc. **75**, 493 (1992).
[35]Y. Fu and A. G. Evans, Acta Metall. **33**, 1515 (1985).
[36]H. Gao, L. Zhang, W. D. Nix, C. V. Thompson, and E. Arzt, Acta Mater. **47**, 2865 (1999).
[37]X. Zeng, Z. Du, C. A. Schuh, and C. L. Gan, MRS Commun. **7**, 747 (2017).
[38]C. L. Cramer, P. Nandwana, R. A. Lowden, and A. M. Elliott, Addit. Manuf. **28**, 333 (2019).
[39]M. Cologna, B. Rashkova, and R. Raj, J. Am. Ceram. Soc. **93**, 3556 (2010).
[40]J. G. Santanach, A. Weibel, C. Estourns, Q. Yang, C. Laurent, and A. Peigney, Acta Mater. **59**, 1400 (2011).
[41]R. E. Chinn, *Ceramography: Preparation and Analysis of Ceramic Microstructures* (ASM International, 2002).
[42]E. D. Whitney, Trans. Faraday Soc. **61**, 1991 (1965).
[43]R. C. Garvie and M. V. Swain, J. Mater. Sci. **20**, 1193 (1985).
[44]M. M. R. Boutz, A. J. A. Winnubst, and A. J. Burggraaf, J. Eur. Ceram. Soc. **13**, 89 (1994).
[45]J. R. Heffelfinger and C. B. Carter, Surf. Sci. **389**, 188 (1997).
[46]C. Herring, Phys. Rev. **82**, 87 (1951).
[47]J. R. Heffelfinger, M. W. Bench, and C. B. Carter, Surf. Sci. **343**, L1161 (1995).
[48]J. E. Bonevich and L. D. Marks, J. Mater. Res. **7**, 1489 (1992).
[49]W. W. Mullins, Philos. Mag. **6**, 1313 (1961).
[50]M. Kurumada, H. Hara, and E. Iguchi, Acta Mater. **53**, 4839 (2005).
[51]P. Mondal, Solid State Ionics **118**, 331 (1999).